Supporting information

Plasmon-Induced Photoelectrochemical Water Oxidation Enabled by *In-situ* Layer-by-Layer Construction of Cascade Charge Transfer Channel in Multilayered Photoanode

Zhiping Zeng,[a#] Tao Li,[a#] Yu-Bing Li,[a#] Xiao-Cheng Dai,[a] Ming-Hui Huang,[a] Yunhui He,[b] Guangcan Xiao,[b] Fang-Xing Xiao[a]*

a. College of Materials Science and Engineering, Fuzhou University, Fuzhou, 350002, People's Republic of China.

b. Instrumental Measurement and Analysis Center, Fuzhou University, Fuzhou, 350002, People's Republic of China.

# These authors contributed equally to this work.

*Email - fangxing2010@gmail.com

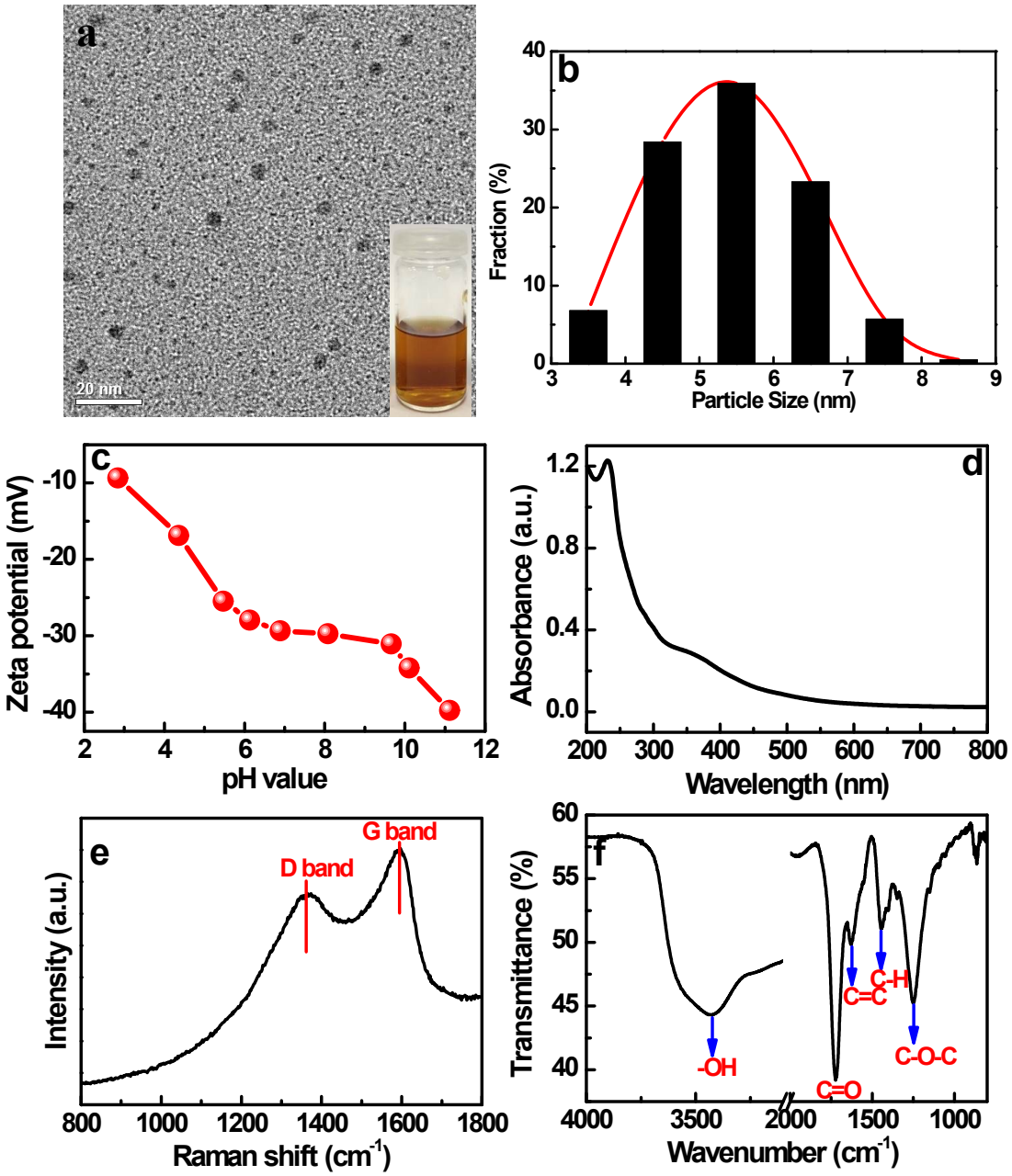

Fig. S1. (a) TEM image of GOQDs with corresponding graph in the inset and size histogram in (b), (c) zeta potential result, (d) UV-vis absorption, (e) Raman and (f) FTIR spectra of GOQDs.

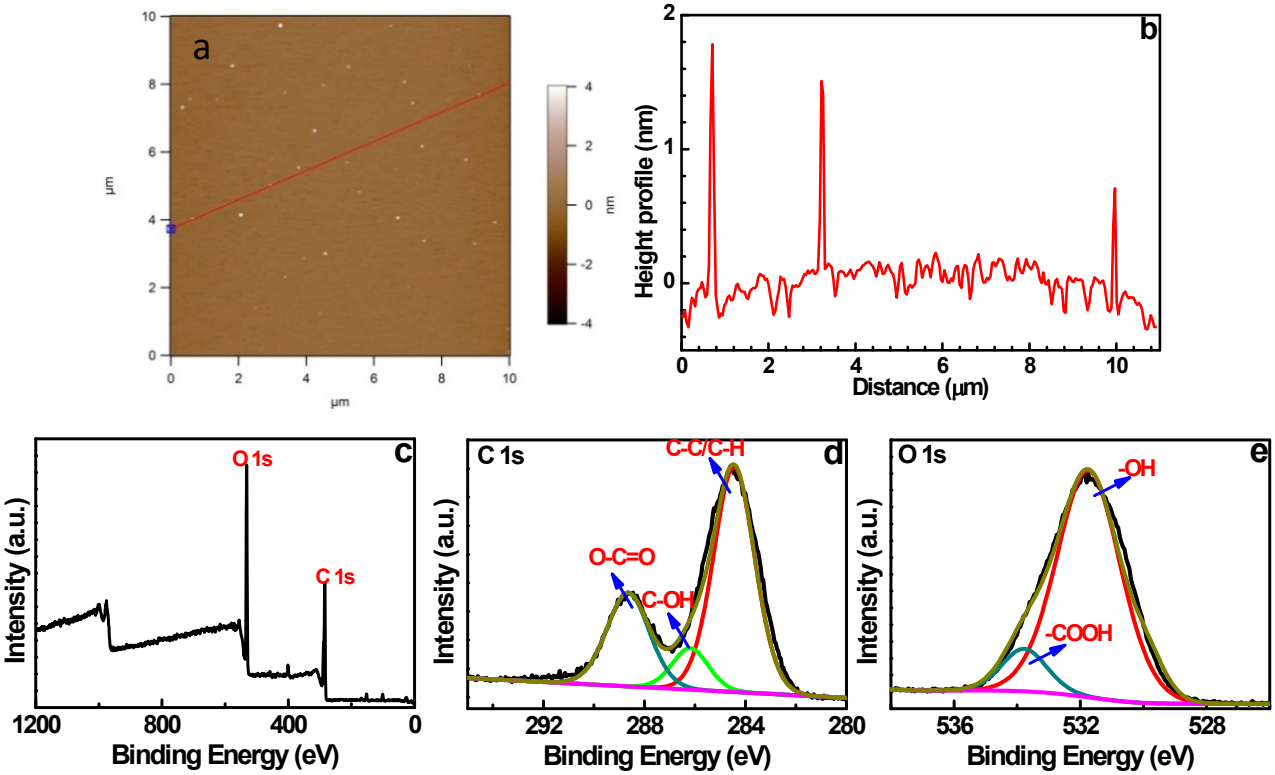

Fig. S2. (a) AFM image of GOQDs with corresponding height profile in (b), (c) survey spectrum and high-resolution (d) C 1s and (e) O 1s spectra of GOQDs.

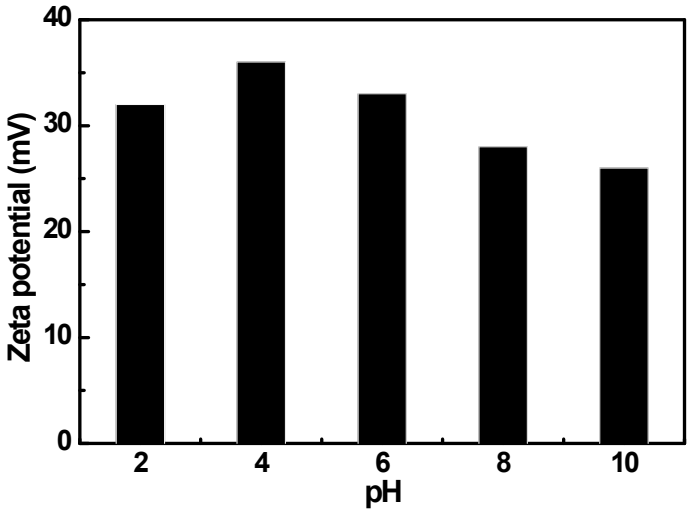

Fig. S3. Zeta potential of PEI-Ag^{+} complex.

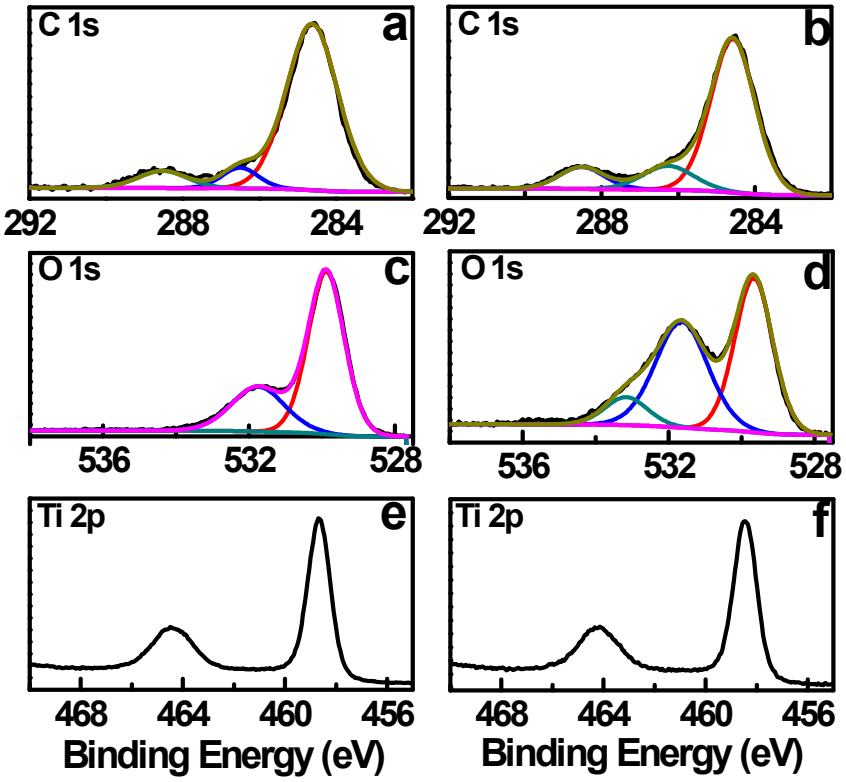

Fig. S4. High-resolution (a & b) C 1s, (c & d) O 1s, and (e & f) Ti 2p spectra of (a, c, e) pristine TiO_2 NRs and (b, d, f) TiO_2 NRs@Ag@GQDs heterostructure.

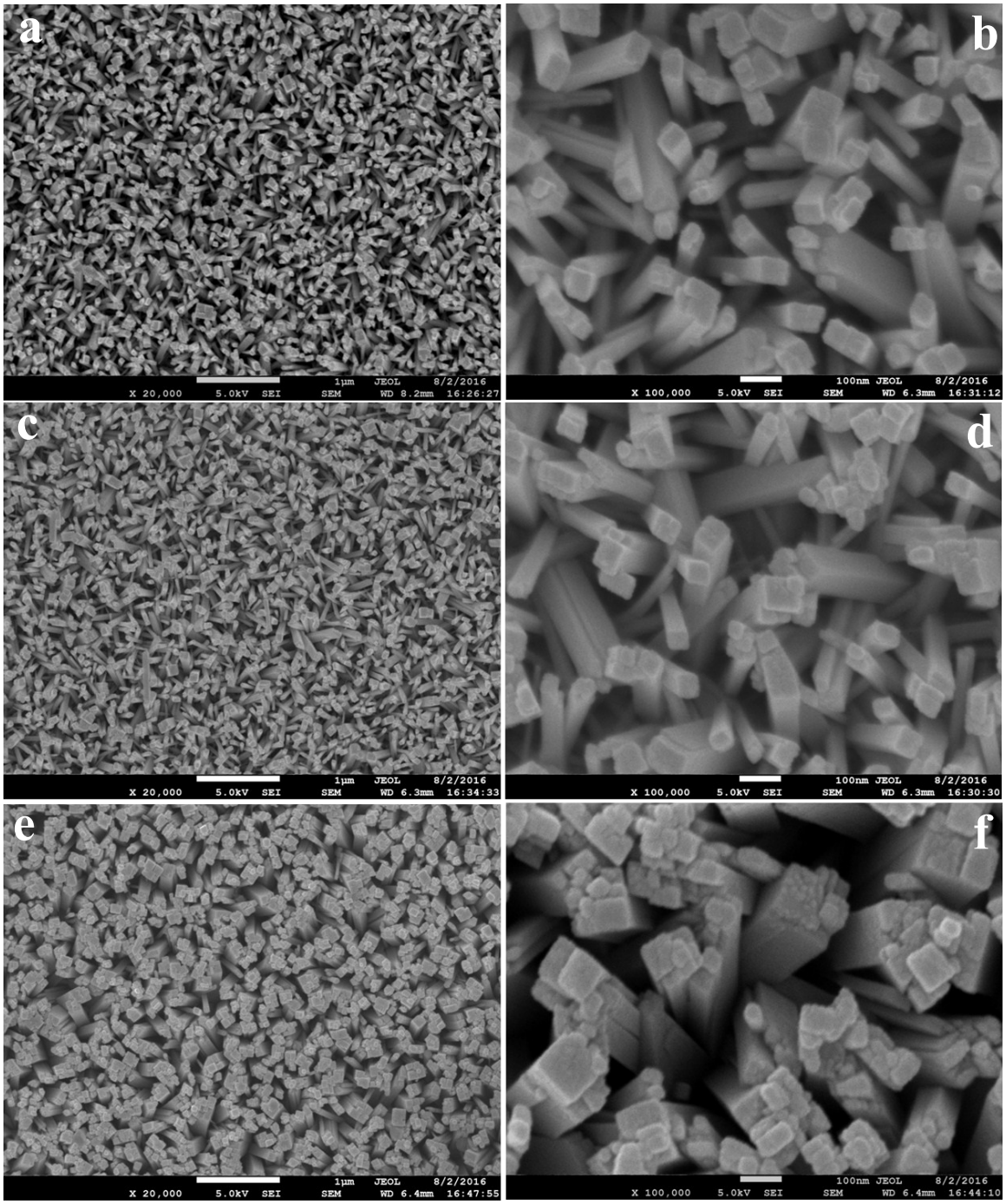

Fig. S5. Low and high-magnified panoramic FESEM images of (a & b) pristine TiO_2 NRs, (c & d) TiO_2 NRs@GQDs binary and (e & f) TiO_2 NRs@Ag@GQDs ternary heterostructures.

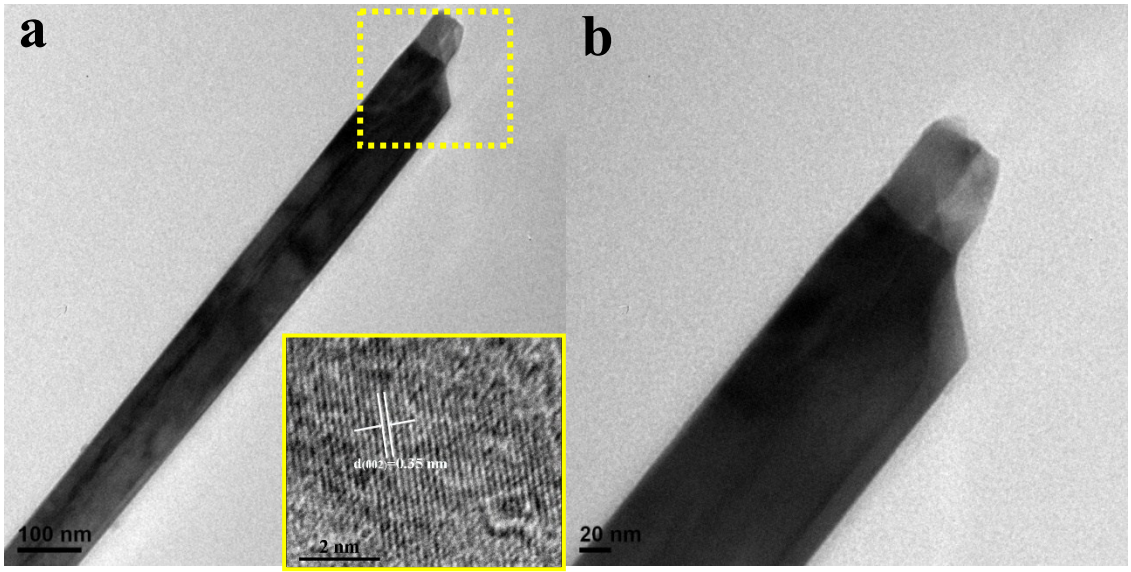

Fig. S6. (a) Low and (b) high-magnified TEM images of pristine TiO_2 NRs with corresponding HRTEM image in the inset of a.

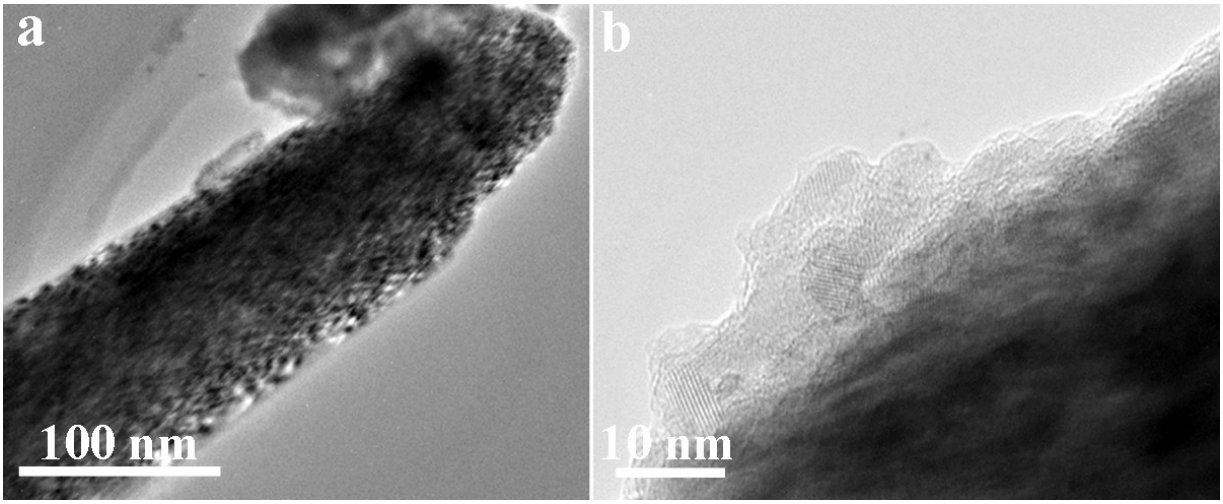

Fig. S7. (a) TEM and (b) HRTEM images of TiO_2 NRs@GQDs heterostructure.

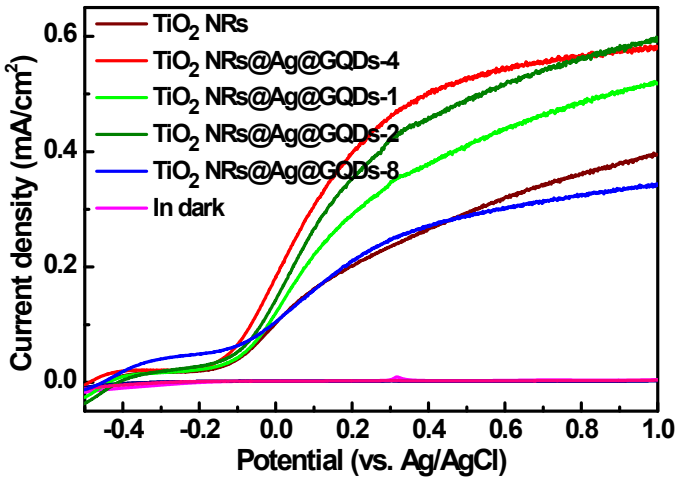

Fig. S8. (a) LSV results of pristine TiO_2 NRs and TiO_2 NRs@Ag@GQDs with different assembly cycles under simulated solar light irradiation (AM 1.5G, 0.5 M Na_2SO_4, pH=7).

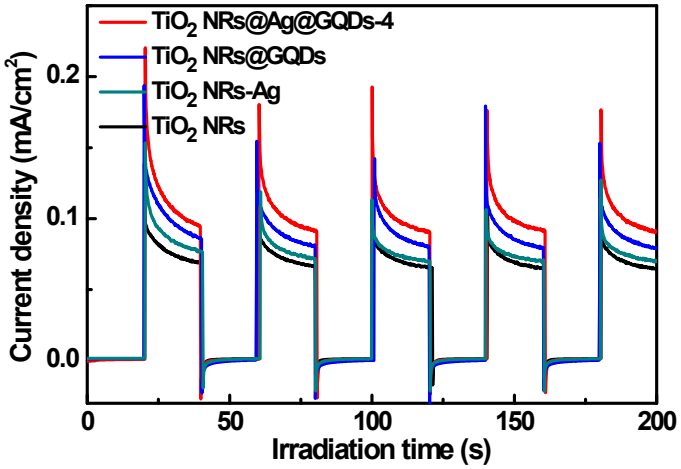

Fig. S9. On-off transient photocurrent responses of TiO_2 NRs@GQDs, TiO_2 NRs-Ag and TiO_2 NRs@Ag@GQDs heterostructures under simulated solar light irradiation (AM 1.5G, 0.5 M Na_2SO_4, pH=7, bias: -0.1 V vs. Ag/AgCl).

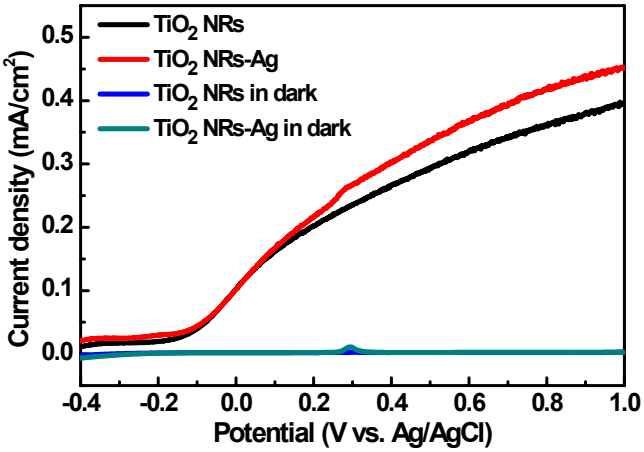

Fig. S10. LSV results of pristine TiO_2 NRs and TiO_2 NRs-Ag under simulated solar light irradiation (AM 1.5G, 0.5 M Na_2SO_4, pH=7).

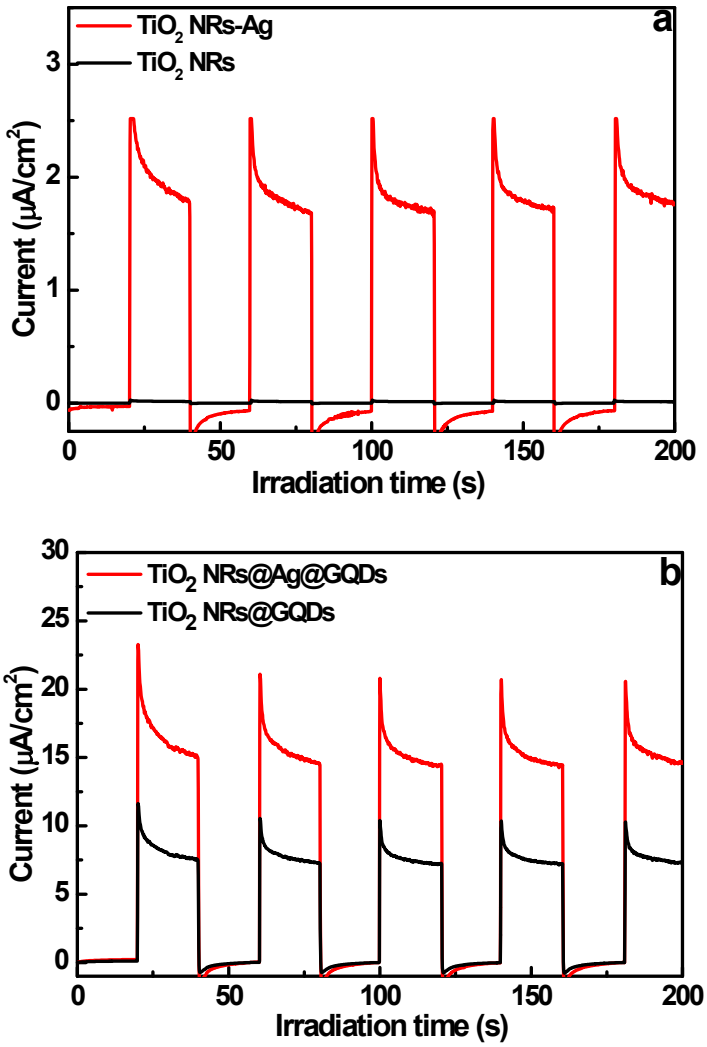

Fig. S11. Comparison on the on-off transient photocurrent responses between (a) pristine TiO_2 NRs and TiO_2 NRs-Ag as well as photocurrent comparison between TiO_2 NRs@GQDs and TiO_2 NRs@Ag@GQDs under visible light irradiation (λ>400 nm, 0.5 M Na_2SO_4, pH=7).

Note: It is apparent in **Fig. S11a** that pristine TiO_2 NRs exhibits negligible photocurrent under visible light irradiation owing predominantly to its large band gaps; however, TiO_2 NRs-Ag demonstrates pronounced photocurrent under the same conditions and this can only be ascribed to the plasmonic excitation of Ag NPs leading to the production of hot charge carriers (hot electrons). They are able to flow to the conduction band of TiO_2, thereby resulting in the generation of photocurrent under visible light irradiation albeit the photon energy is lower than the band-gap-photoexcitation energy of TiO_2. **Fig. S11b** shows that TiO_2 NRs@Ag@GQDs demonstrates significantly enhanced visible-light-driven photocurrent in comparison with TiO_2 NRs@GQDs, once again highlighting the pivotal role of Ag NPs in boosting the production of plasmon-induced hot carriers.

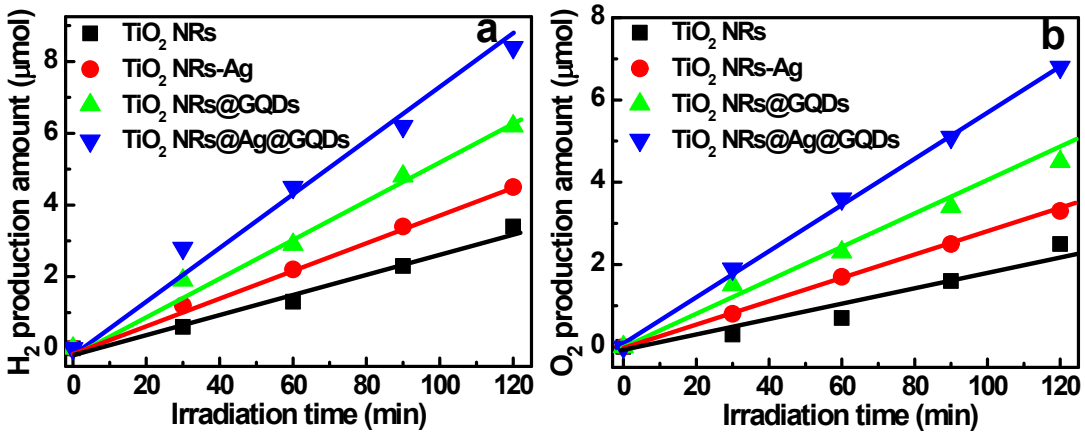

Fig. S12. (a) Hydrogen and (b) oxygen production amount of different photoanodes under continuous simulated solar light irradiation (AM 1.5G, 0.5 M Na_2SO_4, pH=7) for 2 h at a bias of 1.23 V vs. RHE.

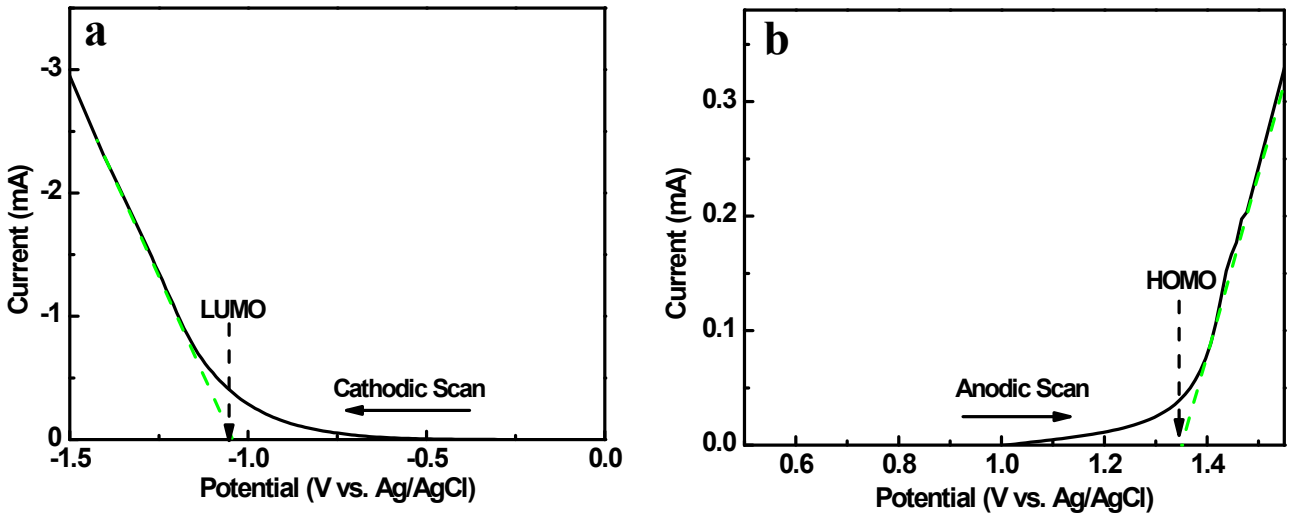

Fig. S13. (a) LUMO and (b) HUMO energy levels of GQDs determined by a cathodic and anodic scan (5 mV/s) method.

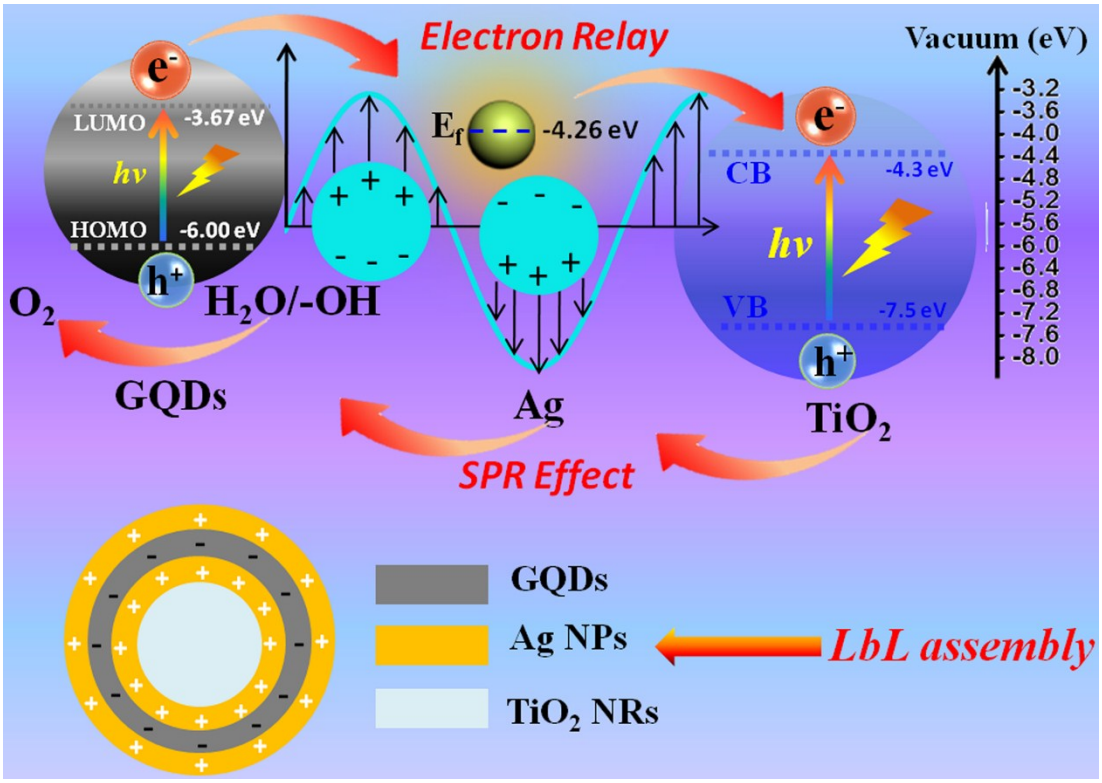

Scheme S1. Schematic illustration of PEC water splitting mechanism over TiO_2 NRs@Ag@GQDs ternary heterostructure.

2. Experimental section

2.1 Preparation of graphene quantum dots (GQDs)

Graphene oxide quantum dots (GQDs) were prepared with CX-72 carbon black via being refluxed in a concentrated nitric acid (HNO_3) solution.[1,2] Typically, 0.4 g dried CX-72 carbon black was added to 6 mol L^{-1} nitric acid (100 mL) and refluxed for 24 h at 110 ºC. After cooling to below 30 ºC, the product was centrifuged (12000 rpm) for 10 min to achieve a sediment and a supernatant. The resultant supernatant was treated at 200 ºC to evaporate the nitric acid and water. After cooling to room temperature, a reddish-brown solid was acquired. Finally, GQDs aqueous solution was obtained by dissolving GQDs in DI H_2O under 10 min sonication.

2.2 Preparation of TiO_2 nanorod arrays (TiO_2 NRs)

TiO_2 nanorod arrays (TiO_2 NRs) on transparent conductive FTO substrate were synthesized by a hydrothermal growth method.[3,4] In a typical synthesis, FTO substrates were first cleaned with acetone, ethanol, and DI H_2O for 5 min, respectively, and then dried by N_2 stream. The precursor was prepared by adding 0.45 mL of titanium butoxide (97 %, Aldrich) to a well-mixed solution containing 15 mL of HCl and 15 mL of DI H_2O, and then the whole mixture was stirred for another 10 min until the solution became clear. Afterwards, the precursor solution was poured into a Teflon-liner stainless autoclave (50 mL) with the FTO substrates placed at an angle against the wall with the conductive side facing down. Hydrothermal growth was conducted at 150 ^oC for 12 h in an electric oven. Finally, the FTO substrate were rinsed with DI H_2O and dried in ambient air.

2.3 Layer-by-layer assembly of TiO_2 NRs/GQDs andTiO_2 NRs/Ag/GQDs heterostructures

TiO_2 NRs substrate was firstly dipped into polyethylenimine (PEI) aqueous solution (1.0 mg mL^{-1}, 0.5 M NaCl, pH=7) for 10 min and washed three times with DI H_2O, followed by drying with a gentle stream of N_2. Subsequently, the resultant substrate was immersed in GOQD aqueous suspension (1.0 mg mL^{-1}, pH=7) for 10 min, rinsed with DI H_2O, and dried by a stream of N_2. The above procedure as a whole was designated as

a single assembly bi-layer. Multilayered deposition of GOQDs on TiO_2 NRs was achieved by repeating the dipping cycle. Finally, the LbL assembled GOQDs/TiO_2 NRs heterostructures were calcined in an argon atmosphere at 400 ^oC for 1 h at a heating rate of 5 ^oC min^{-1}. For the typical preparation of PEI-Ag^+ complex aqueous solution of a 1:6 concentration ratio of Ag^+ to the repeating unit of PEI, 50 mL of 0.02 mol L^{-1} $AgNO_3$ aqueous solution was slowly added into 50 mL of 5.0 g L^{-1} PEI aqueous solution at pH =9.0 under stirring. The mixture solution was then stirred for 1 h, driving completion of the coordination reaction. Generally, as one Ag^+ ion can coordinate with two amino groups, it is deemed that all the Ag^+ ions can be changed into the coordinating form with PEI.[5] The synthetic process of TiO_2 NRs@Ag@GQDs heterostructure is analogous to TiO_2 NRs@GQDs other than replacing PEI-Ag^+ complex with PEI.

2.4 Characterization

Crystal structure was explored by X-ray diffraction (Brucker D8, 40 kV, 40 mA) using Cu Kα as the radiation source. Transmission electron microscopy (TEM) and high-resolution (HR) TEM images were collected by a JEOL model JEM 2010 EX instrument (200 kV). UV-vis diffuse reflectance spectra (DRS) were obtained on a UV-vis-NIR spectrometer (Varian Cary 500 Scan) using $BaSO_4$ as the background. X-ray photoelectron spectroscopy (XPS) spectra were collected on a photoelectron spectrometer (ESCALAB 250, Thermo Fisher Scientific), binding energy (BE) of the element was calibrated based on the BE of carbon (284.60 eV). Morphology was probed by field emission scanning electron microscopy (FESEM, JEOL JSM6701F). Fourier transform infrared (FTIR) spectra were recorded on a PerkinElmer FTIR spectrometer. Photoluminescence (PL) spectra were collected by an LP920-KS instrument. Atomic force microscopy (AFM, MFP3D, Asylum Research) images were taken by a silicon cantilever, which operates in a tapping mode. Dynamic light scattering analysis (Zeta PALS, Brookhaven Instruments Co.) was used to determine the Zeta potential. Raman spectra were collected on a RenishawinVia Raman System 1000 using an excitation source of 633 nm under ambient conditions.

2.5 Photoelectrochemical water splitting measurements

PEC measurements were carried out on an electrochemical workstation (Zennium, Zahner). The electrochemical setup is composed of conventional three-electrodes, a quartz cell containing 20 mL Na_2SO_4 (0.5 M) aqueous solution and a potentiostat. A platinum plate (20 mm × 10 mm) was used as counter electrode and Ag/AgCl as reference electrode. The samples film (20 mm × 10 mm) were vertically dipped into electrolyte and irradiated with a 300 W Xenon arc lamp (Newport) equipped with an AM 1.5 filter. Monochromatic incident photo-to-electron conversion efficiency (IPCE) spectra were collected using three-electrode without bias, for which monochromatic light was provided by a 300 W xenon arc lamp (Newport) combined with a monochromator (Newport).

References

1 Z. Zeng, F. -X. Xiao, X. Gui, R. Wang, B. Liu and T. T. Y. Tan, *J. Mater. Chem. A*, 2016, **4**, 16383-16393.

2 Z. Zeng, F. -X. Xiao, H. Phan, S. Chen, Z. Yu, R. Wang, T. -Q. Nguyen and T. T. Y. Tan, *J. Mater. Chem. A*, 2018, **6**, 1700-1713

3 F. -X. Xiao and B. Liu, *Mater. Horiz.*, 2014, **1**, 259-263

4 B. Liu and E. S. Aydil, *J. Am. Chem. Soc.*, 2009, **131**, 3985-3990

5 Y. Zhou, R. Ma, Y. Ebina, K. Takada and T. Sasaki, *Chem. Mater.*, 2006, **18**, 1235-1239.